
A NEW CRITERION FOR INTERPRETING ACOUSTIC EMISSION DAMAGE SIGNALS IN CONDITION MONITORING BASED ON THE DISTRIBUTION OF CLUSTER ONSETS

Emmanuel Ramasso^{1*}, Martin Mbarga Nkogo¹, Neha Chandarana², Gilles Bourbon³, Patrice Le Moal³, Quentin Lefèbvre⁴, Martial Personeni³, Constantinos Soutis⁵, Matthieu Gresil⁶

¹*SUPMICROTECH, Université de Franche-Comté, CNRS, institut FEMTO-ST, F-25000, Besançon, France

²Bristol University, Department of Aerospace Engineering, United Kingdom

³Université de Franche-Comté, CNRS, institut FEMTO-ST, F-25000, Besançon, France

⁴Université de Franche-Comté, Institut FEMTO-ST, F-25000, Besançon, France

⁵Department of Materials, The University of Manchester, Manchester, UK & Aerospace Research Institute, The University of Manchester, Manchester, UK

⁶i-Composites Lab, Department of Materials Science and Engineering & Department of Mechanical and Aerospace Engineering, Monash University, Clayton, VIC, Australia

*emmanuel.ramasso@femto-st.fr

ABSTRACT

Structural Health Monitoring (SHM) relies on non-destructive techniques such as Acoustic Emission (AE) which provide a large amount of data over the life of the systems. The analysis of these data is often based on clustering in order to get insights about damage evolution. In order to evaluate clustering results, current approaches include Clustering Validity Indices (CVI) which favor compact and separable clusters. However, these shape-based criteria are not specific to AE data and SHM. This paper proposes a new approach based on the sequentiality of clusters onsets. For monitoring purposes, onsets indicate when potential damage occurs for the first time and allows to detect the initiation of the defects. The proposed CVI relies on the Kullback-Leibler divergence and enables to incorporate prior on damage onsets when available. Three experiments on real-world data sets demonstrate the relevance of the proposed approach. The first benchmark concerns the detection of the loosening of bolted plates under vibration. The proposed onset-based CVI outperforms the standard approach in terms of both cluster quality and accuracy in detecting changes in loosening. The second application involves micro-drilling of hard materials using Electrical Discharge Machining. In this industrial application, it is demonstrated that the proposed CVI can be used to evaluate the electrode progression until the reference depth which is essential to ensure structural integrity. Lastly, the third application is about the damage monitoring in a composite/metal hybrid joint structure. As an important result, the timeline of clusters generated by the proposed CVI is used to draw a scenario that accounts for the occurrence of slippage leading to a critical failure.

Keywords Clustering Validity index · Acoustic Emission · Clusters timeline · Structural Health Monitoring

1 Introduction

Acoustic emission (AE) is a non-destructive technique developed to monitor materials during mechanical tests. The data are collected through highly sensitive sensors able to detect subnanometric displacements at the surface of a material. These displacements occur due to the propagation of stress waves generated by the formation of damage within the material/structure. Therefore, the AE technique is widely used as inputs of expert systems to get insights about the

behaviour of a material or a structure under stress [1]. Due to the lack of knowledge concerning the precise source of each AE signal, expert systems take the form of unsupervised learning workflows [2, 3] based on three main steps in order to interpret AE data (Figure 1).

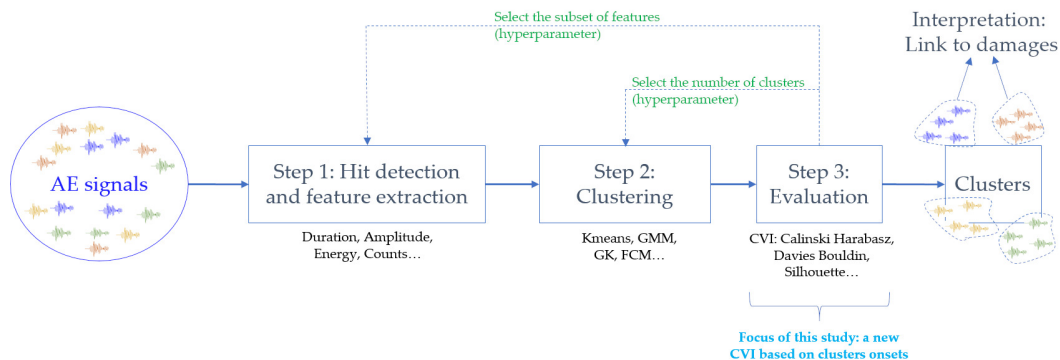


Figure 1: Feature-based clustering of AE data.

During experimental campaigns, AE data are collected in the form of a data stream acquired between 1 and 10 MHz. The stream is made up of AE transients mixed with noise. The first processing step includes wave-picking in order to detect discrete AE signals (also called AE hits) that are deemed to be relevant (i.e. not noise) for interpreting the material behavior [4, 5, 6, 7]. Each AE signal is traditionally transformed into a d -dimensional feature vector that represents a basis with the same number of dimensions and axes for all signals. Some dozens of features are generally extracted [8] due to a lack of knowledge about the optimal subset of features to be used. The features are represented by a $N \times d$ matrix that feeds into the clustering algorithm applied in the second step. The goal of clustering is to create K groups of feature vectors called clusters. The clustering step involves hyperparameters (the algorithm's parametrisation), which play a role in the convergence but can not be optimised through the objective function used to find the clusters. Two critical hyperparameters are generally involved in AE data clustering: the choice of the features and the choice of the number of clusters.

In the standard approach for AE data clustering, these hyperparameters are generally set according to an algorithm detailed in A which includes the third step, called validation. This step makes use of a criterion (or a combination of criteria) to evaluate the quality of the clustering result according to the hyperparameters. In pattern recognition, these criteria are also called Clustering Validity Indices (CVI) [9]. Following [10, 2], several indices (line 14) can be computed for all parametrisations ($k \cdot C_n^p$ for subsets of p features from n and considering k different numbers of clusters). Then a majority voting scheme, relying on some weighting provided by the end-user, selects the best number of clusters and the best subset of features (lines 19-24).

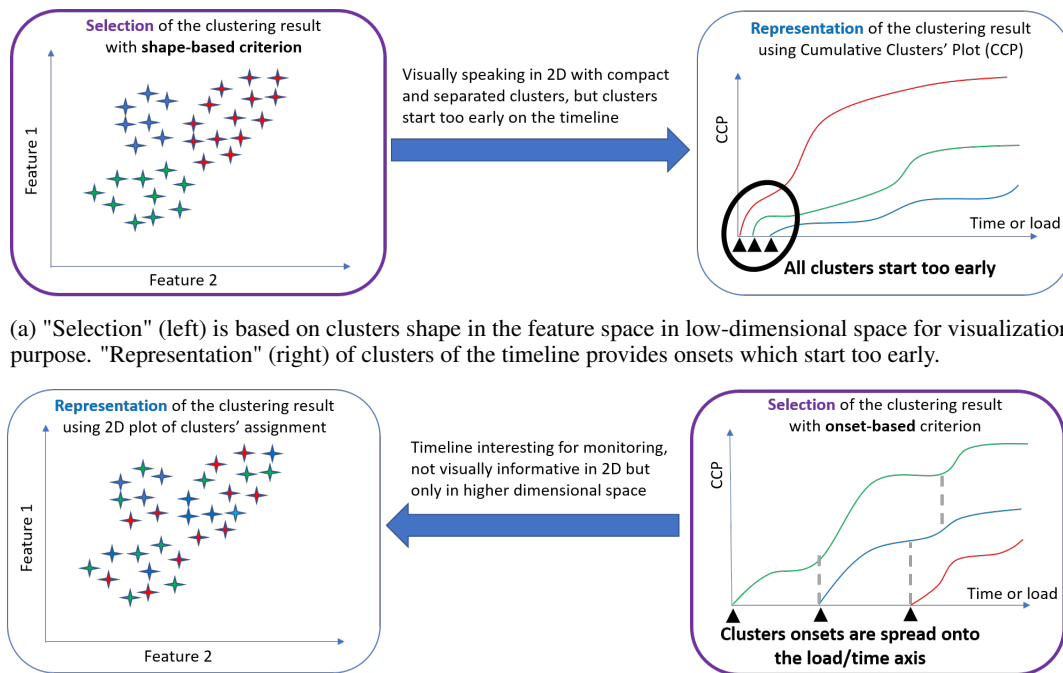
“Quality” in clustering is a subjective notion. For decades, researchers interested in AE data clustering have focused on finding “natural” clusters. A natural cluster was defined in 1968 by J. W. Carmichael, R. S. Julius [11] as “(1) a relatively densely populated regions of the space, and (2) surrounded by continuous and relatively empty regions of the space”. Given this definition *related to the shape and compactness of clusters* in the feature space, the clustering of AE data sets collected during mechanical tests is generally posed as finding a set of hyperparameters such that natural clusters are obtained. For that, *internal* CVI are almost exclusively used to evaluate to what extent a set of clusters is natural for a given AE data set. An internal CVI takes the features and the parameters of the clusters (e.g. centers) as inputs, in addition to some hyperparameters involved in the clustering method (for example, the type of distance between feature vectors). It then generates a real value that reflects the quality of the clustering result. In AE literature, Davies-Bouldin [12] and Silhouette criteria [13] are often used. By focusing on *clusters’ shape*, these CVI foster clustering results made of compact and well-separated clusters.

As an alternative to focusing on clusters’ shape for the validation of clustering results, several publications were recently focused on the development of algorithms for finding relevant clusters in terms of *sequence, timeline* or *chronology*. For example, a visualization of AE events in geoscience was suggested in [14] where the authors determined the 3D location through time of each AE event, similar to locating the focus of an earthquake. Similarly, an approach integrating spectral analysis of AE waveforms was proposed in [15, 16] aiming at identifying friction and wear mechanisms during degradation of lubricants and contacting surfaces in tribological tests. The authors focused on the chronology of damages and their approach based on supervised learning was shown to simplify the presentation of AE results for quick interpretation. Some other authors did not use clustering but cumulated features in order to visually interpret AE signals and to evaluate damage progression. Cumulated features generally represents a monoparametric interpretation

of AE signals and is a different approach compared to clustering-based analysis which is multivariate [17]. Another drawback of cumulated features is their physical meaning. Moreover, the cumulated values can hide some AE signals which are of low amplitude but frequent and can represent the initiation of late damages.

The idea behind these methods is that damage mechanisms do not usually start simultaneously but according to a timeline: One is often the precursor of the others and damage follows a progression, as known from physics [18], [19, Chap. 6]. *In terms of data science dedicated to AE data, to our knowledge, there is no formal definition of a CVI that allows to select the best parametrisation of a clustering method using onsets of clusters.* Assuming that materials under stress degrade progressively, previous publications shown that such a CVI can be useful for onset-based interpretation of AE. A focus on the timeline of clusters can provide insights into how damages progressively occur and develop. It can inform about the dynamic process involved in the generation of AE signals, which may be relevant to better understand the material behavior and can be used for structural health monitoring purpose [20, 21, 22].

Therefore, our contribution is the formulation of a new CVI for interpreting AE signals based on the distribution of clusters onsets and its validation on three applications. In order to illustrate the positioning of our contribution, Figure 2 depicts the fundamental *difference between shape-based and onset-based approaches* for the evaluation of AE data clustering results. With the former approach (top subfigures), clusters may be compact and separated in a low-dimensional feature space, but are not ensured to lead to relevant onsets. For example several of them can start very early and almost simultaneously in the data. For monitoring purposes, the latter approach aims at finding subsets of features that point out onsets distributed through the horizontal axis (load or time) which is more helpful to interpret the dynamic behavior of the material or structure under test (bottom subfigures).



(a) "Selection" (left) is based on clusters shape in the feature space in low-dimensional space for visualization purpose. "Representation" (right) of clusters of the timeline provides onsets which start too early.

(b) "Selection" (right) is based on clusters onsets. The timeline is relevant for monitoring. The "representation" (left) in low-dimension (2D in general) of the clusters can be useless because the clusters are compact and separated only in higher dimensions (used in clustering). The compactness and separation of clusters is ensured during clustering.

Figure 2: Selection and representation of clusters results.

Section 2 introduces the proposed criterion for selecting the best parametrisation. It is evaluated in Section 3 using a benchmark obtained from a real structure. This benchmark allows us to quantify whether the criterion drives the end-user to a better interpretation compared to standard approaches.

2 Sorting subsets of features with respect to onsets

The AE data are supposed to be made of N d -dimensional feature vectors $\mathbf{x}_n \in \mathbb{R}^d$. Given a subset of features $S \subset \mathbb{R}^d$ and a number of clusters K , a partition P is obtained by a clustering method. P is represented by a vector of length N , where each element $P(n) \in \{1, 2 \dots K\}$ represents the cluster number assigned to each AE signal. For fuzzy clustering methods, $P(n)$ is the cluster with the largest membership degree.

A cluster's onset is defined as the first occurrence of the cluster. For example, for cluster k , the onset is the first index in P where the k -th cluster appears. Onsets can be represented on an axis related to time, load or any physical quantities related to the degradation of the material. Illustrations can be found on the right hand-side of Figure 2 and on Figure 3.

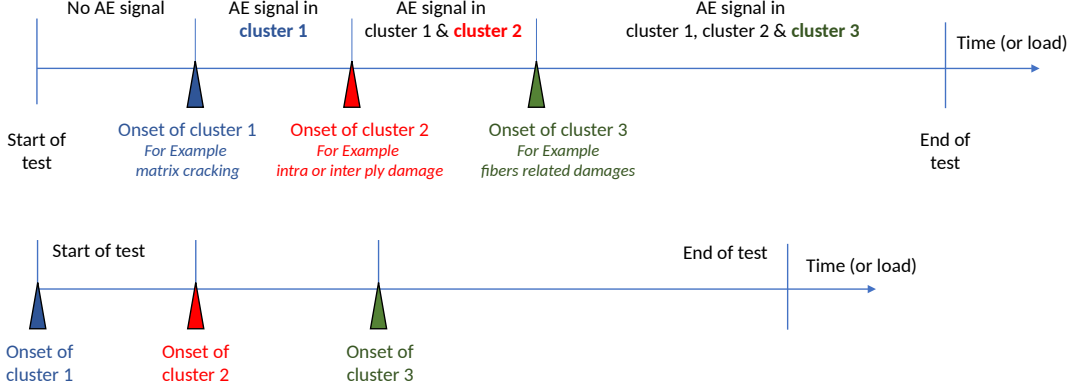


Figure 3: Illustration used in examples in Section 2: Onsets (triangles) are defined as the first occurrence of each cluster. The horizontal axis can be any monotonically increasing information regarding the evolution of the test like, for example, time or a damage variable. In-between onsets, several clusters, that previously occurred, can keep growing. Reference to composite damages is only for illustration. Top figure: No signal appears from the beginning to the first onset so this part is removed and the starting time shifted accordingly, which leads to the bottom figure.

Let's define $t_k \in [0, T]$ as the first occurrence of cluster k in a data set (with the first onset starting at $t_1 = 0$). Using onsets, we compute the normalised difference between two consecutive onsets as

$$\Delta_k = \frac{t_{k+1} - t_k}{T} \quad t_{K+1} = T \quad (1)$$

The set $\mathbf{p}_{\text{est}} = \{\Delta_k\}_{k=1}^K$, estimated by clustering, can be interpreted as a probability distribution made of K elements since we have

$$\sum_{k=1}^K \Delta_k = 1 \quad (2)$$

Example 1. As an example, consider Figure 3. We have three clusters, with onsets positioned, for example, at $t_1 = 27, t_2 = 57, t_3 = 82$ and with $T = 127$ (horizontal axis is with arbitrary unit, in practice it can be related to time, load or a physical quantity). We can shift the onsets to get $t_1 = 0, t_2 = 30, t_3 = 55$ and $T = 100$. Then $\Delta_1 = 30/T, \Delta_2 = 25/T, \Delta_3 = 45/T$, satisfying Eq. 2. In that case, $\mathbf{p}_{\text{est}} = [0.30, 0.25, 0.45]$.

2.1 Case 1: A priori onsets is available

Let's first assume that the end-user can provide the expected onsets (composed of K values). This prior onsets can, for example, be provided by a physics-based model able to predict the onset of each damage or cluster. In that case, we have a piece of information about onsets that should be taken into account to select the clustering parametrisation. These preexisting onsets can be represented as a distribution, say \mathbf{p}_{true} , following the same reasoning as before. The problem is now to compare \mathbf{p}_{true} (the prior distribution) and \mathbf{p}_{est} (the estimated distribution).

The degree of agreement between estimated onsets and the ground truth as quantified by \mathbf{p}_{est} and \mathbf{p}_{true} respectively, can be evaluated by different means, for example using the L_1 norm, the Hellinger distance, the Bhattacharyya distance, the total variation distance between probabilities, the Kullback-Leibler (KL) or Renyi divergences, among others. The KL divergence is used in the present work. KL is *not symmetric* and *never negative* and was used in many machine learning algorithms based on probability theory and on artificial intelligence. In information theory, KL is the amount

of information lost when one distribution (for example, depending on parameters) is used to approximate another (for example, related to a ground truth). We compute the KL divergence as follows:

$$KL(\mathbf{p}_{\text{est}}||\mathbf{p}_{\text{true}}) = \sum_{k=1}^K \mathbf{p}_{\text{est}}(k) \log_2 \left(\frac{\mathbf{p}_{\text{est}}(k)}{\mathbf{p}_{\text{true}}(k)} \right) \quad (3)$$

In this expression, \mathbf{p}_{est} is dependent on S , the subset of features used for clustering, and K the number of clusters. The KL is thus made of two terms. First, a cross entropy loss

$$CE(\mathbf{p}_{\text{est}}||\mathbf{p}_{\text{true}}) = - \sum_{k=1}^K \mathbf{p}_{\text{est}}(k) \log_2 (\mathbf{p}_{\text{true}}(k)) \quad (4)$$

and, second, Shannon's entropy

$$E(\mathbf{p}_{\text{est}}) = - \sum_{k=1}^K \mathbf{p}_{\text{est}}(k) \log_2 (\mathbf{p}_{\text{est}}(k)) \quad (5)$$

with $KL = CE - E$.

2.2 Case 2: Without a priori on onsets

Even though some initial onsets could be obtained numerically (by simulations) or experimentally (for example using infrared thermography or strain sensors), it is more frequent, in practice, to be in the situation where there is no a priori on onsets of clusters. Therefore, how to set \mathbf{p}_{true} without a priori? Since \mathbf{p}_{true} is a distribution, one answer is to make use of the *principle of maximum entropy*. It consists in not adding unconscious arbitrary assumptions and avoid introducing biases other than those that are already present in the data [23, 24]. Therefore, *in absence of a priori on onsets, among all possible distributions of onsets for \mathbf{p}_{true} , we should select the one with the largest entropy which corresponds to the uniform distribution.*

When using the uniform distribution of onsets for \mathbf{p}_{true} in CE (Eq. 4), we get

$$\mathbf{p}_{\text{true}} = \text{Uniform} \Rightarrow CE(\mathbf{p}_{\text{est}}||\mathbf{p}_{\text{true}}) = - \log_2 \frac{1}{K} = \log_2 K \quad (6)$$

which means that KL tends to:

$$\mathbf{p}_{\text{true}} = \text{Uniform} \Rightarrow KL(\mathbf{p}_{\text{est}}||\mathbf{p}_{\text{true}}) = \log_2 K - E(\mathbf{p}_{\text{est}}) \quad (7)$$

We can simplify Eq. 7 by dividing by $\log_2 K$ leading to

$$\frac{1}{\log_2 K} KL(\mathbf{p}_{\text{est}}||\mathbf{p}_{\text{true}}) = 1 - E_{\text{norm}}(\mathbf{p}_{\text{est}}) \quad (8)$$

where $E_{\text{norm}} \in [0, 1]$ is the normalized entropy of \mathbf{p}_{est} . Therefore, for a given K , minimizing the initial criterion in Eq. 3 divided by $\log_2 K$ is equivalent to maximizing the entropy of onsets. A possible criterion to sort subsets is thus:

$$Q_{\text{proposed}}^{\text{ONSETS}}(S, K) : \quad \text{Given } K, \text{ find } \arg \max_S [E_{\text{norm}}(\mathbf{p}_{\text{est}}(\cdot|S, K))] \quad (9)$$

where it is made explicit that E depends on K (the number of clusters) and S (subsets of features). Therefore, for a given K , the criterion is used to sort the subsets according to the distribution of the onsets.

Example 2. Let us continue the previous example: with $T = 100$, and with $K = 3$ we can define three onsets distributed uniformly in order to define \mathbf{p}_{true} , located at $t_1^{\text{true}} = 0$, $t_2^{\text{true}} = T/3 = 33.33$, $t_3^{\text{true}} = 2T/3 = 66.66$, with all $\Delta_k = 33.33/T$. Therefore $\mathbf{p}_{\text{true}} = \mathbf{p}_{\text{uniform}} = [0.33, 0.33, 0.33]$ (at two digits of precision, the sum must be one). Using \mathbf{p}_{est} of the previous example, we get $KL = 0.0454714$ (Eq. 3) with $CE = 1.585$ and $E = 1.539$. The maximum of E for 3 clusters is $\log_2(3) = 1.585$ therefore $E_{\text{norm}} = 1.539/1.585 = 0.971$.

Remark 1. One important point to observe is that the proposed CVI only requires the partition, not the features conversely to shape-based CVI. Therefore, according to [25], the proposed criterion belongs to the family of "external" CVI whereas shape-based are said "internal". However, the proposed criterion is a particular case because external CVI actually require a complete reference partition to be compared with, meaning that the ground truth must be known for all feature vectors, whereas the proposed CVI only requires the onsets of clusters.

2.3 Proposed algorithm

The algorithm based on onsets for evaluating clustering results of AE data is presented in Alg. 2 (Appendix B). In this algorithm, $Q_{\text{proposed}}^{\text{ONSETS}}(S, K)$ used in line 10 is given by Eq. 9 and has to be maximized. In line 12, partitions are sorted according to the value of this criterion and a few dozens of the best ones are selected. For example, the value of the first percentile of the values of $Q_{\text{proposed}}^{\text{ONSETS}}$ can be used to determine the number of partitions to be selected. For each selected partition, the onsets are determined (line 15) by simply finding the time of the first occurrence of each cluster. These steps are done for each number of clusters, separately.

Finally, *onsets are stacked independently on the number of clusters* and the result is presented by means of a histogram that approximates the distribution of onsets. Results of the accumulation of onsets are presented to the end-user who visually determines the position of onsets by analyzing the peaks at some places in the histogram. As in interactive clustering [26], based on the histogram, the end-user can then either reject, accept, or be ignorant of the result, triggering a re-clustering of the data, for example using different features or another clustering method.

The histogram can be interpreted as follows:

- High peaks mean that varying the number of clusters and features lead to similar locations of onsets. According to the application, this can reflect a robustness of the clustering method or its inability to decompose the data set into clusters.
- Many small peaks mean that a change of the number of clusters implies a systematic change of the location of onsets. In that case, the clustering method is not robust or the features are not relevant.
- In real AE data sets, it is expected to get high peaks located at various locations surrounded by smaller peaks. It means that some clusters are found with different onsets but varying the number of clusters or the features implies a variability on the onsets.
- Since the first cluster starts at 0 by construction (Eq. 1) for all features and all clusters, the first peak will be the highest and represents the number of combinations selected to plot the histogram.

The location of the peaks can be helpful for the end-user to conclude that some damages potentially start or grow from these locations or if the clustering is meaningful or not.

3 Experiments

Three applications have been considered. Table 1 present the details about their parametrisation such as the number of features per subset, the possible number of clusters and the clustering method. For each application, the results of the proposed onset-based CVI (Alg. 2) and CVI based on clusters' shape [10] (Algorithm 1) are presented.

Table 1: Applications used to illustrate the proposed criterion. GMM stands for Gaussian Mixture Model, GK for Gustafson-Kessel, EDM for Electrical Discharge Machining.

Application	# sensors used	Total # features	# features per subset	# clusters	Ground truth	Clustering method
Bolted metallic structure	1	19	4	{2, 3, 4 . . . 10}	Yes (7 classes)	Kmeans
EDM μ -drilling hard material	1	26	3	{4, 6, 8, 10}	No	GK
Glued Hybrid tubular structure	4	19	3	{4, 6, 8, 10}	No	GK

3.1 Data set #1: Monitoring of a bolted metallic structure

3.1.1 Setup and data description

The benchmark data set ORION-AE is presented in [27]. In this data set, the true labels are provided which allowed us to evaluate the performance of the proposed criterion and compare it with the standard solution. The data were collected on a setup designed to reproduce the loosening phenomenon observed in aeronautics, automotive or civil engineering structures where parts are assembled together by means of bolted joints (Figure 4).

The benchmark is composed of different campaigns of measurements. In the following, the set of measurements called “*measurementSeries_B*” (campaign #B) was used for illustration. The structure was submitted to a 120 Hz harmonic

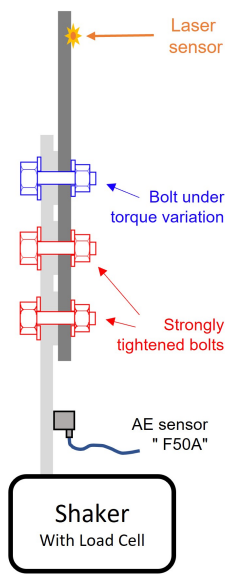


Figure 4: Setup configuration for ORION-AE application.

excitation force. Seven tightening levels were applied on the upper bolt, starting from 60 cNm (set with a torque screwdriver) and held during a 10-seconds vibration test. The shaker was stopped and this vibration test was repeated after a torque modification at 50 cNm. Torque modifications at 40, 30, 20, 10 and 5 cNm were then applied in this order. In each campaign, three sensors are available and we used the AE sensor named “F50A” for illustration. The raw data are illustrated in Figure 5. From the raw data (green), *the goal is to infer the tightening levels by clustering and to compare the results with the ground truth* (blue stairs).

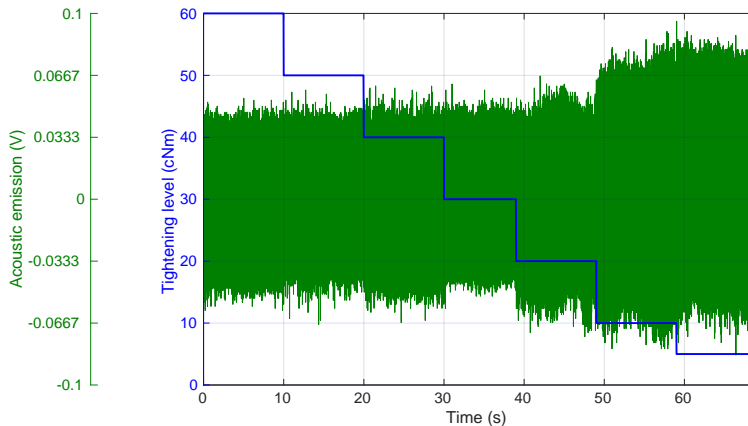


Figure 5: Raw data (green) and tightening levels (in blue represented by stairs).

The features are freely available at the following link [27]: https://drive.google.com/drive/folders/1H413RxYu4ya7YMEgF_1Th_fHr7f1vv00?usp=sharing. They are common features used in the AE community [28]: Rise time, counts, counts to peak, duration, MARSE and absolute energies, amplitude, average signal level, signal strength, RMS, reverberation frequency, initiation frequency, average frequency, partial power in [0,200], [200,400], [400,600], [600,1000] kHz, peak frequency and centroid frequency. The set of feature vectors was post-filtered using a 31-sample moving median applied to each dimension in order to ensure temporal coherence, and one point over three were kept in order to reduce the amount of points (there are about 1200 cycles per tightening levels in the original data set).

3.1.2 Parametrization of algorithms

Algorithms 1 and 2 were used on every combination of 4 features within the set of 19 mentioned above, so leading to 3876 combinations for each $K = 3, 4 \dots 10$ value with a total of 31008 combinations. Kmeans clustering method was run 5 times for every combination and the result leading to the minimum sum of squared euclidean distances over all points and clusters was selected. If an empty cluster was obtained, the corresponding subset of features was not used. For Algorithm 1 (based on shape), the voting scheme proposed in [10] was applied. We used three internal CVI implemented in Matlab's Statistical and Machine Learning Toolbox, namely: Silhouette, Calinski-Harabasz and Davies-Bouldin. We used the same 25 points voting scheme as in [10]. Algorithm 1 was applied for each K independently in order to sort the subsets of features and select the best one. For Algorithm 2 (onset-based), the 20 best partitions were selected for each number of clusters using the onset-based CVI.

3.1.3 Link between clusters onsets and change in tightening levels

We evaluated whether the clusters' onsets coincide with the changes of tightening levels. For that, we represented the distribution of the estimated onsets using histograms. This was done in all partitions found by the previous algorithms and for all numbers of clusters ($K = 3 \dots 10$). Histograms depict the ground truth with blue stairs and the vertical dotted lines represent the instant of the true changes in the tightening level. This ground truth is available in [27]. The stairs show the duration of each level, equal to 10.0, 10.0, 10.0, 9.0170, 10.0, 10.0 and 10.0 seconds for, respectively, 60, 50, 40, 30, 20, 10 and 5 cNm.

Histograms of onsets for shape-based and onset-based CVI are presented in Figure 6 with a bin size of 0.5 s. *These results only differ by the criterion since the same partitions obtained by the Kmeans method were used to evaluate both criteria in the same conditions.* With the shape-based approach (Fig. 8a), we can observe three missing onsets (no vertical bar at 10, 30 and 60 s corresponding to 50, 30 and 5 cNm), one delayed onset (20 s / 40 cNm) and one clear false positive (at around 44 s). *Based on this histogram, an end-user is likely to select 4 clusters, with one wrong and 3 missed tightening levels.*

Figure 8b shows that all changes in tightening levels, except the last one, are detected by the onset-based CVI. Four primary peaks distinctly appear, located at expected times corresponding to changes in tightening levels at 60 cNm (0 s), 50 cNm (10 s), 40 cNm (20 s), 20 cNm (40 s), 10 cNm (50 s). *The same partitions were used in both cases which means that only the CVI makes the difference.* The peak at 30 s is well distinguishable with 17 occurrences. The secondary peaks (lower occurrence) are globally distributed around the main ones and represent the variability on onsets in the 20 partitions. Onset at 60 s corresponding to 5 cNm was not found because of a mixing made by the clustering with the data in the previous tightening level (50 s / 10 cNm).

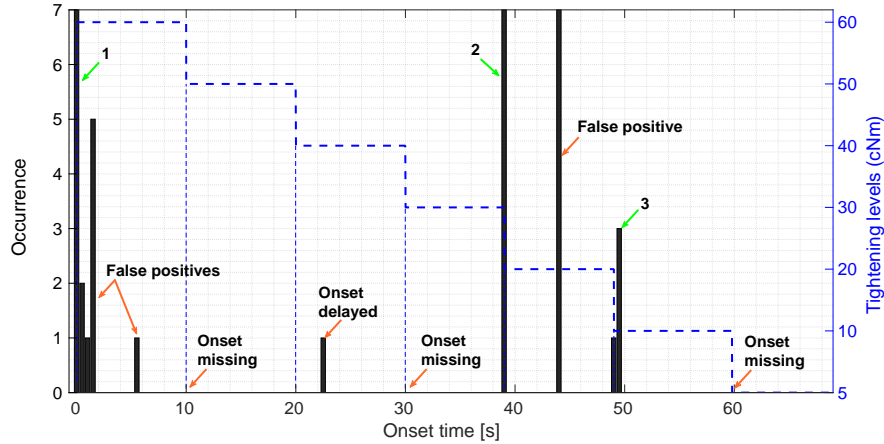
3.1.4 Link between clusters onsets and clusters overall quality

We evaluated whether the content of clusters (over all tightening levels) coincide with the ground truth. For that, the 20 best partitions provided by each criterion were evaluated using the Rand Index (RI) [29]. RI is a value in $[0, 1]$ reflecting the quality of clustering, where "1" means that the assignment of clusters made by clustering is correct for all feature vectors. The number of points in each partition is 4684.

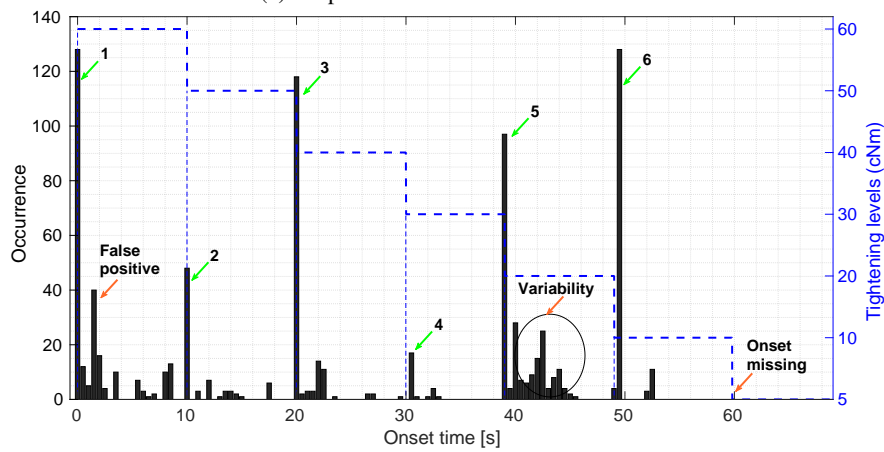
Results are presented in Figure 7 using boxplots. The red line is the median value, and the box is defined by the minimum and maximum whisker length ($W=1.5$ as the default in Matlab) so that RI values are considered as outliers if they are larger than $Q3+W*(Q3-Q1)$ or smaller than $Q1-W*(Q3-Q1)$, where $Q1$ and $Q3$ are the 25th and 75th percentiles, respectively. The outliers are represented with red crosses. The figure shows that, overall, the median RI values are globally close. If we consider values around the ground truth ($K_{true} = 7$), the main difference is the width of the boxes which is largest for the shape-based CVI. This is confirmed in Table 2 which is a summary of the RI values for $K = 6, 7, 8$. The table shows that the minimum RI values are higher for the onset-based with an improvement of 4% to 7%, while the maximum values are similar. We can also see that 4 values are found as outliers below the minimum (and 11 for all values of K) for the shape-based criterion, representing 10% of the results. Conversely, no outlier was detected with the onset-based criterion for $K = 6, 7, 8$ (and 3 for all values of K), demonstrating its higher robustness to the change of features.

3.1.5 Case of a data set with non-uniformly distributed onsets

In ORION-AE data set, the tightening levels have approximately the same duration which is a special case. In this section, we propose to evaluate the proposed criterion when the duration in each tightening level is not similar. For that, we selected only a part of the data in each level so that the duration of the levels follows a non linear evolution. Practically, it means that the metallic plates remain tightened for a longer period for a given level compared to the



(a) Shape-based CVI with the best vote



(b) Proposed onset-based CVI with 20 best partitions

Figure 6: Validation of the clustering provided by a Kmeans using the voting scheme and onset-based criteria.

Nb cluster/perf	min		max		median		nb outliers	
	onset	shape	onset	shape	onset	shape	onset	shape
CVI								
K=6	77.7	72.3	86.2	86.6	81.2	81.7	0	0
K=7	81.0	73.8	86.0	86.0	82.2	83.9	0	2
K=8	81.8	77.0	86.5	87.1	84.1	85.9	0	2

Table 2: Rand index for onset-based and shape-based CVI with K=6,7,8 (± 1 around the ground truth).

subsequent levels. For 60, 50, 40, 30, 20, 10 and 5 cNm, the first seconds of data were kept as follows: 10 s, 8.5 s, 7 s, 5 s, 3 s, 2 s and 1.5 s, and the remaining data were discarded.

The results are reported in Figure 8. We can observe that the proposed onset-based CVI outperforms the standard approach. As in the previous case, only the last onset is not discovered by the onset-based CVI. Conversely, the shape-based criterion found three onsets. For 50 cNm (10 s) and 40 cNm (20 s) only one occurrence is found which not enough to distinguish these onsets from the false positives ones around.

3.1.6 Summary

When averaged over 20 partitions, each made of more than 4800 points, we observed that the quality of clusters found by the onset-based criteria is improved by 4% to 7%. An improvement can also be observed with the proposed onset-based CVI in terms of accuracy and robustness to changes in features and number of clusters. In terms of onsets, a distinct improvement was observed with the onset-based CVI which makes this criterion suitable for structural health monitoring purposes. The results illustrate the interest of this kind of criterion to detect changes in AE data by clustering.

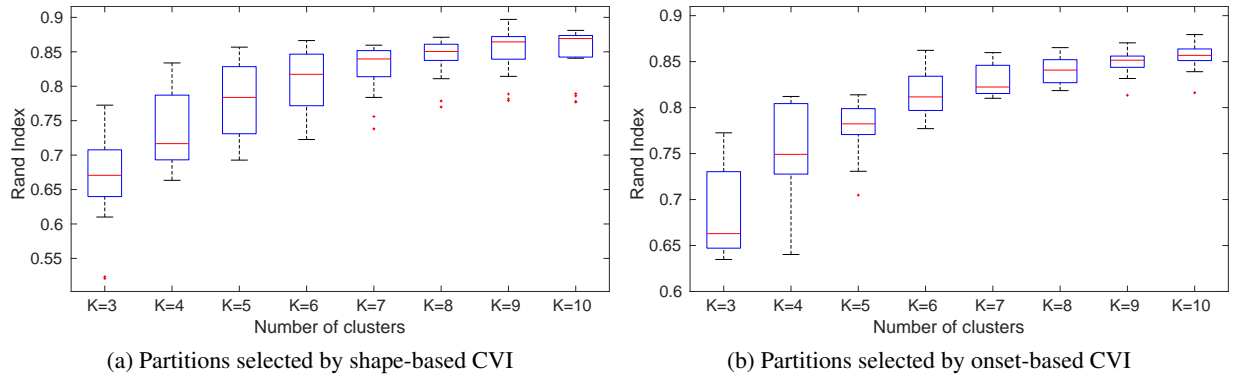


Figure 7: Performance evaluated by the Rand Index

3.2 Data set #2: Monitoring of an electrical discharge machine during microdrilling

This application is about monitoring of a manufacturing process called Micro Electrical Discharge Machining (Micro-EDM) used for drilling micro-diameter and deep holes. The goal of AE clustering is here to get insights about the process, and to evaluate if it is possible to detect when the electrode has reached the end of drilling and if the process proceeds similarly between two drillings.

3.2.1 Materials and method

Micro-EDM relies on electrical discharges emitted by a tool-electrode and used to remove material in a work piece hosed by a dielectric (Fig. 9a). An electric arc is formed between the conducting part and the electrode which are not in contact, making it possible to machine very hard conductive materials with a very high flexibility in terms of shapes machined [30]. Both the feed rate of the tool-electrode and the sequence of discharges, necessary to remove pieces of material to reach a reference in depth, are controlled by a proprietary software. Moreover, during the process, both the work piece and the tool-electrode get damaged and it is difficult and time-consuming to evaluate precisely and in real-time their degree of wear. We therefore used the acoustic emission technique to collect data during drilling with the aim to get insights about the process. More specifically, the goal is to evaluate whether the chronology of acoustic emission signals helps in monitoring the progression of the electrode until the reference depth.

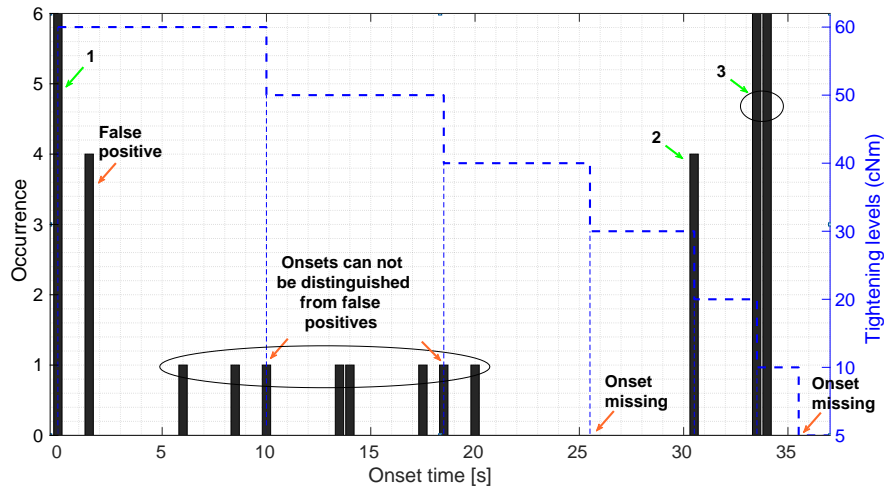
Experiments were conducted on a SARIX EDM machine. The particularity of this machine is the auto-regulation of input parameters for the sparkles generation. A 0.3 mm diameter tubular electrode was used to drill a 2 mm hole opening into a 0.3 mm thick cavity. The drilled material is a Ni-based superalloy. Figure 9b shows the set-up on the EDM machine. The camera is synchronized with the start of the process to record the moment when the electrode starts drilling. The camera is then used to visually evaluate when a sparkle appears in the cavity corresponding to the opening of the hole (3rd image in Figure 9a). This event is noted on the figures below since we expect a particular behavior on the AE signals and clusters.

AE streaming were acquired at a sampling frequency of 5 MHz, using a "micro-80" sensor made by Mistras-EuroPhysical Acoustics, with an operating frequency range in 200-900 kHz. Acquisition of stream data was made using a Picoscope from Picotech. The AE hits were detected using the same method as in application #1 (ORION-AE) and with similar features except the partial powers, considered in the following intervals: in 0-20 kHz, 20-100 kHz, 100-200 kHz, 200-300 kHz, 300-400 kHz, 400-500 kHz, 500-600 kHz, 600-800 kHz, 800-1000 kHz. A total number of 24 features were considered.

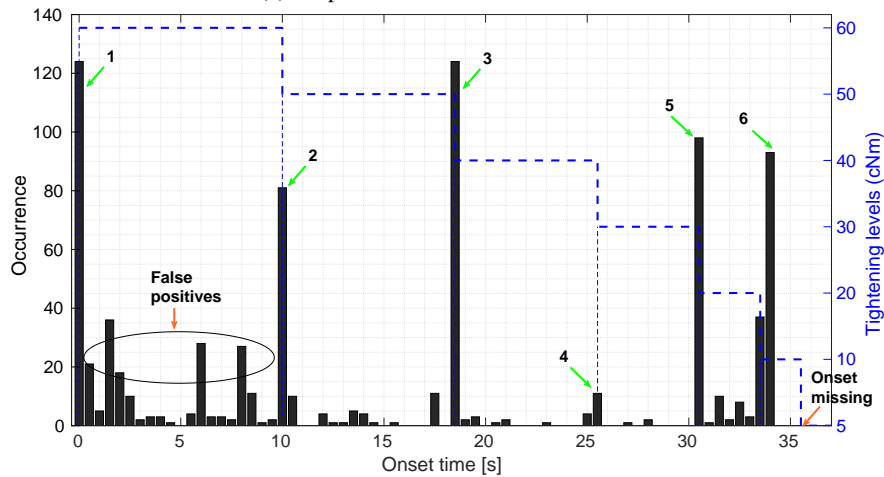
3.2.2 Results

The tests presented below were made using a brand new electrode and after cleaning the machine. Two tests were performed successively. Algorithm 2 (based on onsets) was used on every combination of 3 features within the set of 24 features (total of 2024 combinations). The 20 best partitions found by this algorithm for each number of clusters $K \in \{4, 6, 8, 10\}$ were used to build the histograms.

Histograms are presented in Figure 10 for test #1 (brand new electrode) and test #2 (after one test). In these experiments, the electrode position is not known precisely due to its continuous wear during machining. Therefore, we used the camera to evaluate, approximately, when the first sparkle appears at the opening of the hole into the cavity. Based on the images, we identified the following time instants (depicted on figure 10):



(a) Shape-based CVI with the best vote



(b) Proposed onset-based CVI with 20 best partitions

Figure 8: Case of non-uniform onsets: Validation of the clustering provided by a Kmeans using the voting scheme and onset-based criteria.

- Test #1: The first sparkle after opening the hole appears between 14-15 s and the next surface is drilled from about 17-18 s.
- Test #2: The first sparkle after opening the hole appears at about 18-19 s and the next surface is drilled from about 22-23 s.

The cumulated energy is superimposed on histograms. The energy feature is traditionally extracted from AE signals since it provides some trends about damage evolution.

For test #1 (Fig. 10a), four main stages identified on the histograms are represented by dash-dotted lines. The position of the lines is based on the evolution of the cumulated energy and on the position of onsets of clusters. In stage I (0-6 s), there are three primary peaks and a low energy. They are related to the first appearances of sparkles at the gap distance (defined as the distance between the electrode and the workpiece for which the first sparkles appear). During the process, drilling is performed if a constant gap is ensured between the electrode and part surfaces. However, these surfaces are limited in the first stage, and a few number of sparkles are required until an initial hole is actually made. In Stage II (6-15 s), the cumulated energy increases importantly, in two main phases (6-12 s, 12-15 s) with one primary onset when the slope changes (around 12 s). The changes of the slope in energy during drilling is typical from an adaptation of the machine to find a control law in order to succeed in drilling. At 15 s, Stage III starts, until about 17.6 s, with two primary onsets (number 5 and 6). The rectangle points out this important stage because the beginning of Stage III corresponds to the first sparkle observed on the camera. Therefore, this onset clearly points out that the drilling is

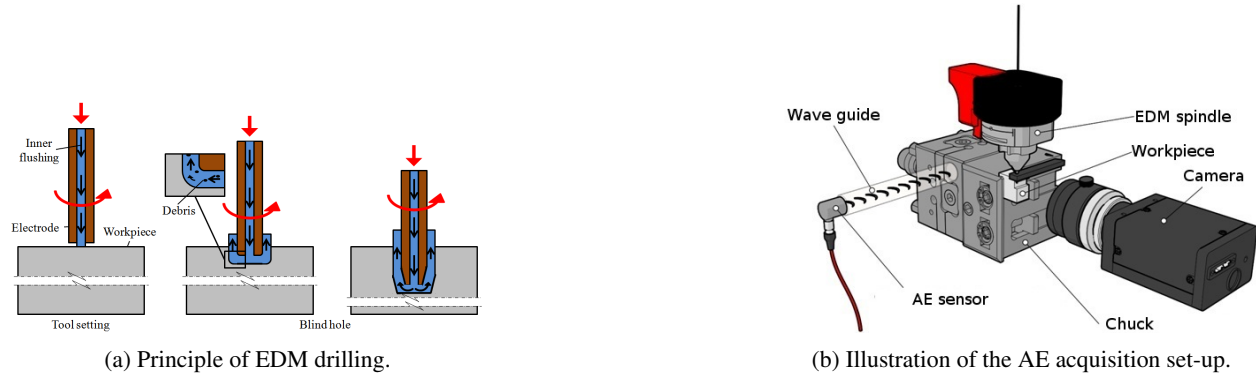


Figure 9: EDM principle and instrumentation [30].

approaching the output of the first part of the workpiece. This rectangle shows that about 2.6 s are needed to finalize the drilling and approaching the surface of the second part of the workpiece. From 18 s onwards (Stage IV), we can see one more onset (number 7) representing the start of drilling of the second part. No more significant onsets appear meaning that the AE signals collected in the second part have similar characteristics as in the first part, likewise the machine was using a similar control law.

For test #2 (Fig. 10b), the length of Stage IV is shorter because the process was able to drill more easily the second part of the workpiece from about 21.5 s. The process is more stable than in the case of test #1 in order to find its control law to succeed in drilling. This is confirmed by a more regular cumulated energy increase until the first sparkle observed with the camera at the opening of the hole. Indeed, test #1 depicted a significant variation of the cumulated energy curve associated to the start of a stable drilling process. In test #2, the drilling process is quite continuous and stable. It can be observed that the left-hand side of the rectangle points out the important phase when the first sparkle occurs (around 18.2 s). Compared to test #1, there is no onset exactly at the same location, but there is one just before (number 7) and one just after (number 8). The latter (within the rectangle) represents the first sparkle after opening the hole in the cavity, occurring around 19.4 s. The end of this important phase (from an industrial point of view) is characterised by one onset (number 9) just before the start of the drilling of the next part (Stage IV).

3.3 Data set #3: Monitoring of an hybrid composite/metal joint structure

The last application is about monitoring of damages in a hybrid composite/metal joint structure by using the AE technique. The proposed criterion is used to evaluate when damages occur and how it grows during loading until the failure of a metal/composite joint.

3.3.1 Materials and method

The studied specimen is a composite tube manufactured by UTC Aerospace Systems with a joint between a composite part and a metal part. The composite part comprised eight plies of filament wound carbon fibre tows, used to form a tube with a nominal internal diameter of 45.2 mm and wall thickness of 4 mm. The tube geometry was selected to target loads within the range of the target aerospace applications of the structure where bonded joints are harder to certify.

The joining technology between the metallic end-fitting and the composite tube is in the form of a bespoke helical thread (screw thread). During the assembly of each joint, an epoxy-based adhesive is applied to the metallic screw thread for lubrication purposes. Preloading of the joint results in the composite being subjected to a through-thickness contact pressure and at the interface, loads are transmitted in two ways: (i) through a reaction force at multiple teeth, and (ii) via friction which results from the predominant contact pressure at flat regions within the bespoke helical thread. If the frictional forces are surpassed, relative movement can occur between the composite and metallic parts of the joint. For this reason, it is of critical importance to the designer to consider both slip and matrix damage. The test of the hybrid joint was designed to prioritise the failure of the interface regions, rather than failing within the composite tube or metallic end fitting.

The specimen was tested in a quasi-static tensile loading configuration on an Instron 5989 electro-mechanical testing machine fitted with a 600 kN load cell. It comprises a composite tube and two metallic end fittings that form two joints, connected to the loading rig via rod ends with spherical bearings, which are screwed into the metallic end fittings. These rod ends were then pinned to clevises that are screwed into the rig. The described test set-up is shown in Figure 11-a).

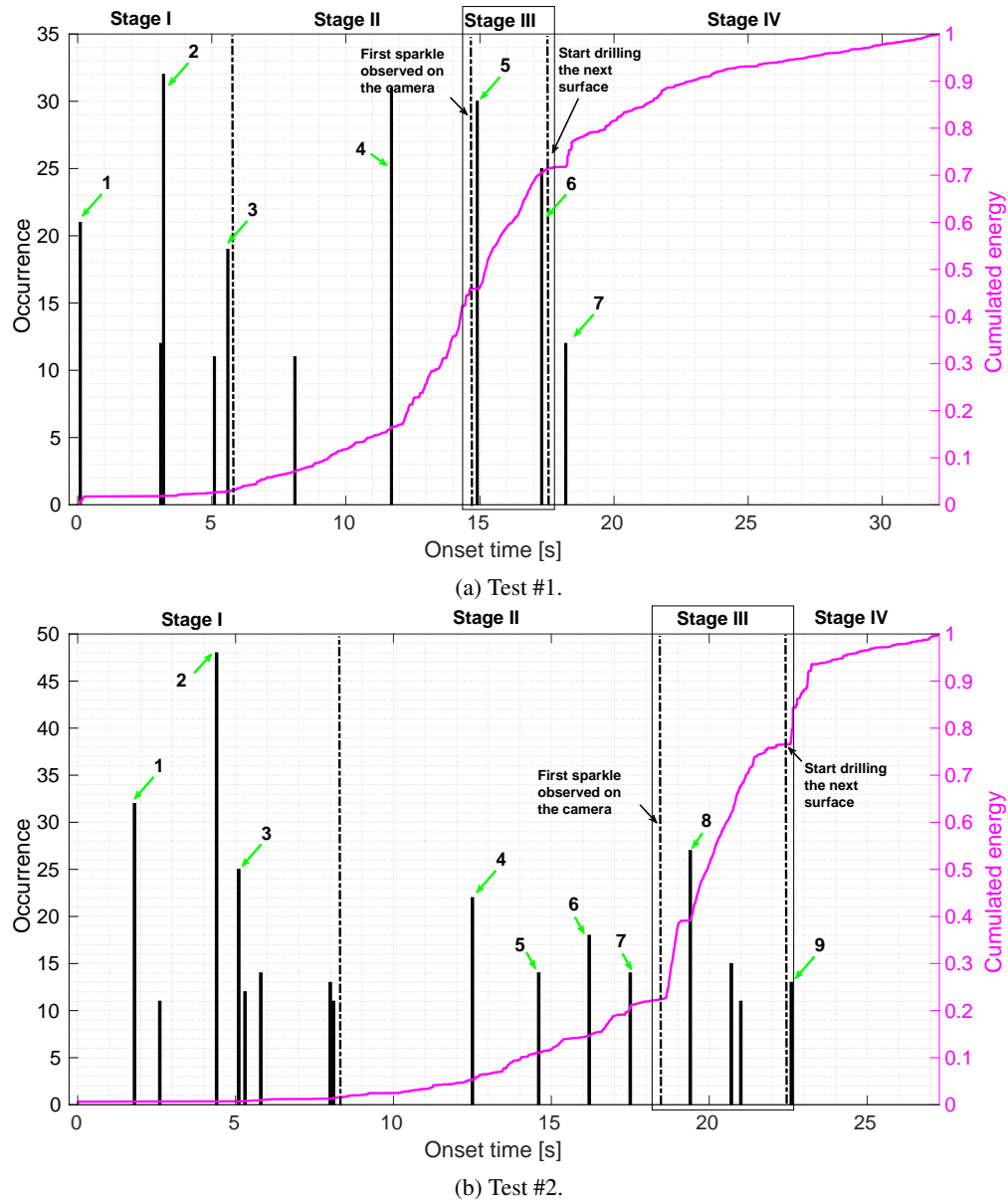


Figure 10: Histogram of onsets (all peaks below 10 are not represented to lighten the figure).

The specimen was loaded at 0.5 mm/min crosshead speed in a single cycle until failure. The specimen failed at the instrumented joint. The breaking loads was 268 kN. The final failure consisted of significant damage caused by initial matrix cracking and followed by slippage at the composite/metal interface of one of the two joints (Figure 11-d) where the screw threads have been almost erased during failure.

Piezoelectric wafer active sensors (PWAS) [31] were bonded to the metal and composite parts of the joint for AE monitoring when the specimen is subjected to quasi-static tensile loading. PWAS of type PIC255, supplied by PI Ceramic-Germany, with 10 mm diameter and 0.5 mm thickness – were used. The positioning of PWAS is shown in Figure 11-b) and c).

AE data were recorded by a PCI-2 based system, and captured in the software "AEWin" (Mistras, USA), with a sampling rate of 10 MHz and 20 dB of pre-amplification per sensor. Hit detection was performed by the software using a threshold of 55 dB and HDT=800 μ s, PDT=200 μ s and HDT=1 ms. In the following, only the data from sensors on the composite part (number 3, 4 on Fig. 11b)) were used for the analysis. The same 19 features as in the first application were used.

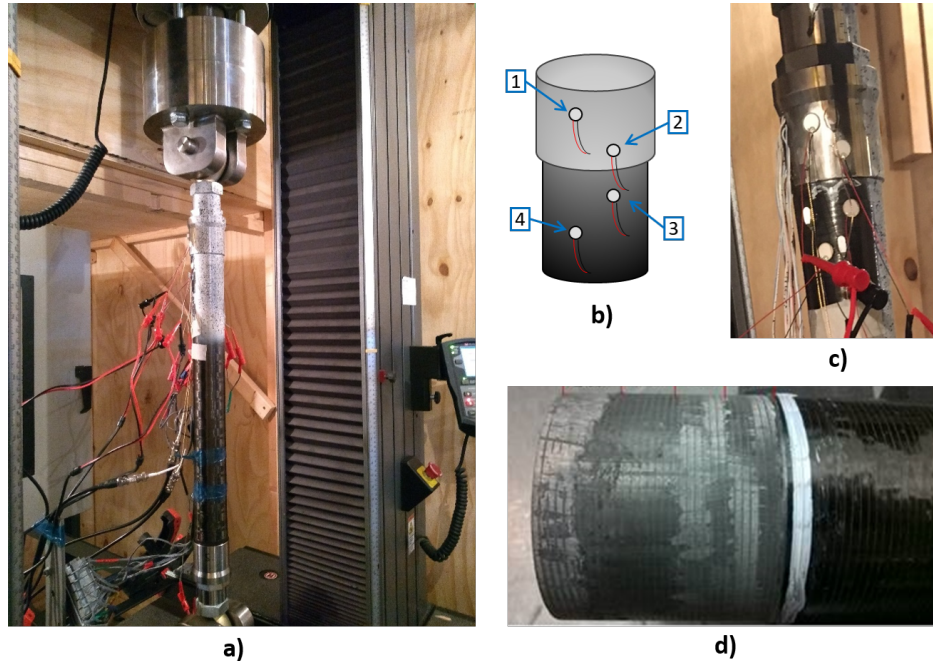


Figure 11: a) Quasi-static tensile loading of the hybrid composite/metal specimens. The specimen is connected to the loading rig at either end via a rod end with spherical bearings that are screwed into the metallic end fittings of the joint. b) and c) Schematic and photograph showing the arrangement of PWAS on both specimens. d) Photograph illustrating final failure of a hybrid composite/metal joint in the form of resin cracking and extensive slippage due to thread crushing. The joint was subjected to quasi-static tensile loading.

3.3.2 Results

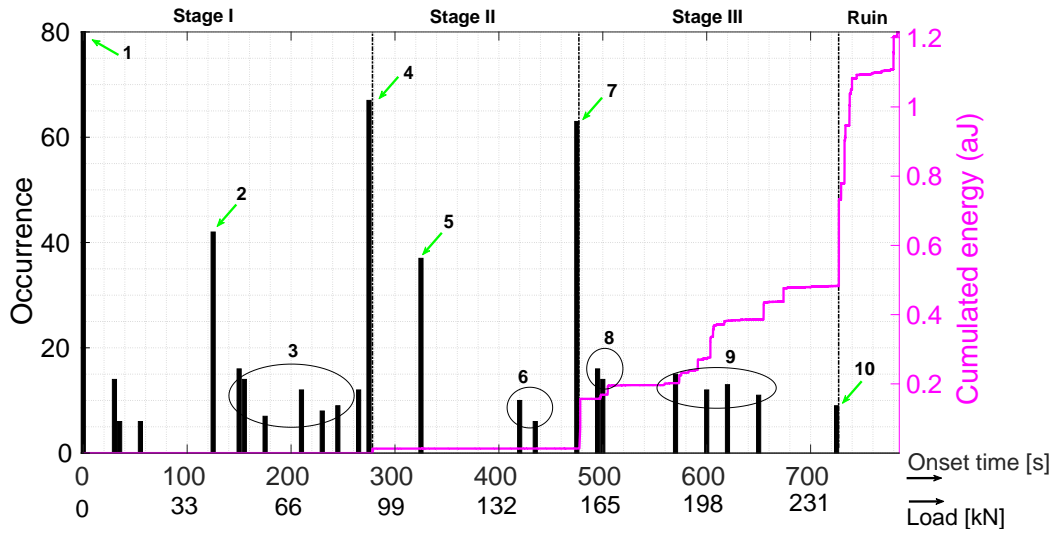
The goal of clustering with onset-based CVI in this application is to determine whether it is able to highlight some phenomenon in a complex engineering structure and if it can help to detect incipient damages within the joint. In many engineering structures, the use of data-driven methods such as clustering is appealing because it can reveal patterns and associations in the data that can help to identify the damage mechanisms. This is particularly of use where the data set is large but also where our predictions and a priori knowledge have a high uncertainty (like with the metal/composite joint). In these cases, the end-user of the AE technique does not have the confidence to assign labels and cannot run supervised algorithms.

In the following, the Gustafson-Kessel clustering method [32] was used in Algorithm 2 by considering all combinations of subsets of 3 features among 19 (so a total of 969 combinations), and varying the number of clusters $K \in \{4, 6, 8, 10\}$ leading to 3876 partitions. The 20 best partitions found by this algorithm for each number of clusters were used to build the histograms represented in Figure 12a. Since we do not have access to a ground truth for this data set, we superimposed the cumulated energy as presented in the previous application and we provided the distribution of amplitudes in clusters for $K = 10$ (Fig. 12b).

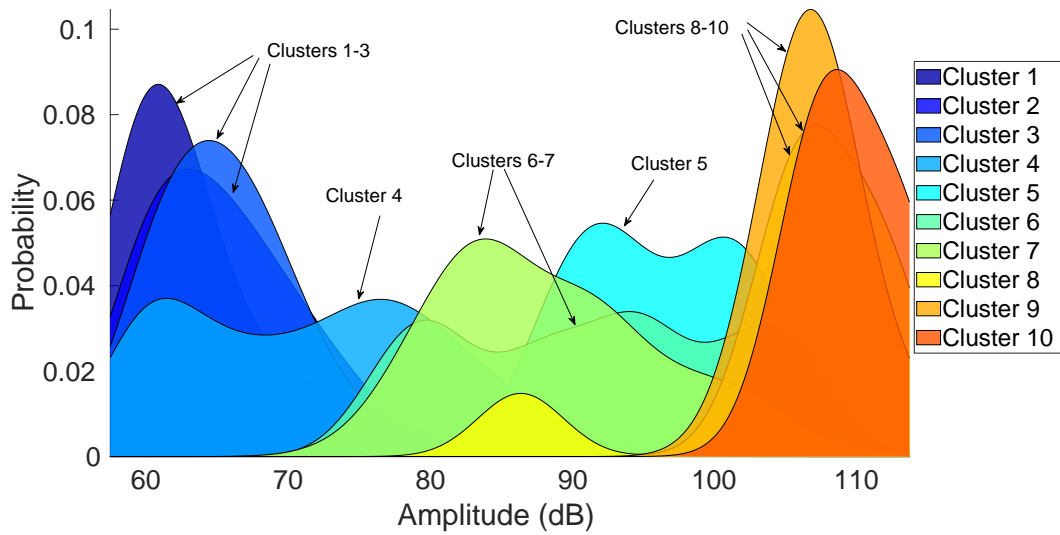
Based on these figures, we can extract three main stages before the ruin. Each stage is characterised by a different evolution of the cumulated energy and different distributions of amplitudes. In the first two stages (0 – 275 s and 265 – 465 s), the cumulated energy shows two plateaus. Actually, there are AE signals during these two periods but their energy is small compared to the signals observed later on, for example during stage III. This is confirmed by Fig. 12b where the first three clusters occurring during stage I depict the lowest amplitudes (55 – 75 dB). Stage II, where onsets 4 – 7 are detected, corresponds to middle range amplitudes (75 – 100 dB). Stage III corresponding to the gradual increase of the cumulated energy is characterised by the largest amplitudes (> 100 db).

The histograms of onsets (Fig. 12a) depicts a primary peak at 270 s. This peak is remarkably close to the first step of increase of the cumulated energy, which corresponds to a sudden release of energetic AE signals. The accumulation of loads during stage I reaches a point that leads to the primary peaks #4 and #5 observed at 265 s and 305 s.

During the plateau 275 – 465 s, few onsets are observed. Since the load is still increasing, it means that previously detected clusters are accumulating until some highly energetic AE signals occurring around 465 s and corresponding to



(a) Histogram of onsets according to time of test and load.



(b) Distribution of amplitudes in clusters.

Figure 12: Analysis of clustering results for the third application.

a new primary peak (#7). The position of this peak is remarkably close to the beginning of the increase of the cumulated energy corresponding to the starting point of a cascade of damages until failure.

A simulation model was developed using Abaqus [33, Chap. 7]. The estimated slip accumulation was found between 90-180 kN, followed by a fatigue period until ultimate failure at 280 kN (compared to 262 kN experimentally). Therefore, according to Figure 12a, slippage can correspond to Stage II found by AE, with clusters #4-8. It corroborates the fact that some damages are described by multiple clusters. Slippage in the joint is indeed a complex phenomenon which can not be described by a unique cluster. The high number of onsets in Stage I, before 265 s (90 kN), together with the low cumulated energy observed in this stage, can be related to friction in the joint when the loads are transmitted at the teeth leading to slippage in Stage II. The accumulation of the loads, which appeared in the two previous stages, starts being critical at 465 s (about 160 kN) corresponding to the fatigue period found by simulation (Stage III in AE data). The clusters found around 600 s (corresponding to 78% of the test duration and 205 kN) are incipient critical damages leading to final failure detected with cluster #10.

4 Conclusion and future works

This study proposes a new approach to interpret acoustic emission data from clustering results. Conversely to standard approaches which favor results with compact and separable clusters, our approach is based on a new Clustering Validation Index (CVI) that put attention on how *onsets* of clusters are distributed on the time/load scales. Onsets reflect the *initiation* of a “defect”, as illustrated in this study by a loosening of a mechanical assembly, a new stage in a manufacturing process or a damage of a composite structure. In most of monitoring applications, this initiation is a very important *characteristic* (in the sense that two distinct defects will generally have different onsets). Therefore, focusing on onsets to interpret AE data can help in monitoring the progression of different damages.

On a benchmark data set, the proposed onset-based CVI outperformed the standard approaches in detecting seven levels of loosening of bolted plates under vibration. The criterion also allowed to detect the changes in the loosening with higher accuracy. These results demonstrate the suitability of the criterion to select the best clustering results without a priori knowledge. Moreover, in case of a priori knowledge is available, the proposed criterion is able to incorporate it which makes it unique compared to standard approaches.

In the second application, data were collected during micro-drilling of hard material using Electrical Discharge Machining. The analysis of the data based on the proposed onset-based criterion allowed us to underline different steps in the process. That paves the way for the control of the quality of the machining through a feedback from acoustic emissions.

The third application concerned the analysis of data collected on a hybrid composite/metal joint. The onset-based criterion allowed us to draw a scenario about the damage occurring within the joint until slippage and failure. Discriminating the onset of the slipping phases leading to failure is essential for Structural Health Monitoring of such hybrid materials.

This work illustrates the need to develop specific tools dedicated to AE data analysis in order to better interpret the behavior of the materials or systems during monitoring. The onset-based criterion is one of these tools and we have shown its relevance on three different applications. As future work, we aim at using this criterion in supervised learning algorithms for Structural Health Monitoring purposes. As shown in experiments, the criterion helps in detecting changes in data which can be exploited to accurately detect incipient defects and to trigger prognostics algorithms. We also aim at developing damage models able to generate onsets of acoustic emission through time or load and to use those a priori onsets in the proposed criterion for improving clustering and classification based on physically-informed algorithms.

Acknowledgement

This work was partly carried out in the framework of the EIPHI Graduate school (contract ANR-17-EURE-0002).

References

- [1] Massimo Bertolini, Davide Mezzogori, Mattia Neroni, and Francesco Zammori. Machine learning for industrial applications: A comprehensive literature review. *Expert Systems with Applications*, 175:114820, 2021.
- [2] Keyla Gonzalez and Siddharth Misra. Unsupervised learning monitors the carbon-dioxide plume in the subsurface carbon storage reservoir. *Expert Systems with Applications*, 201:117216, 2022.

- [3] Carlos Boya-Lara, Omar Rivera-Caballero, and Jorge Alfredo Ardila-Rey. Clustering by communication with local agents for noise and multiple partial discharges discrimination. *Expert Systems with Applications*, page 120067, 2023.
- [4] Jochen H Kurz, Christian U Grosse, and Hans-Wolf Reinhardt. Strategies for reliable automatic onset time picking of acoustic emissions and of ultrasound signals in concrete. *Ultrasonics*, 43(7):538–546, 2005.
- [5] E. Pomponi, A. Vinogradov, and A. Danyuk. Wavelet based approach to signal activity detection and phase picking: Application to acoustic emission. *Signal Processing*, 115:110 – 119, 2015.
- [6] Ramin Madarshahian, Paul Ziehl, and Juan M. Caicedo. Acoustic emission bayesian source location: Onset time challenge. *Mechanical Systems and Signal Processing*, 123:483 – 495, 2019.
- [7] Thang Bui Quy and Jong-Myon Kim. Crack detection and localization in a fluid pipeline based on acoustic emission signals. *Mechanical Systems and Signal Processing*, 150:107254, 2021.
- [8] S. Kattis. Noesis: Advanced data analysis, pattern recognition & neural networks software for acoustic emission applications. In *Kolloquium Schallemission, Statusberichte zur Entwicklung und Anwendung der Schallemissionsanalyse*, Fulda, 9-10 March 2017. Deutsche Gesellschaft für Zerstörungsfreie Prüfung e.V.
- [9] Bernard Desgraupes. Clustering indices. *University of Paris Ouest-Lab Modal’X*, 1:34, 2013.
- [10] M. Sause, A. Gribov, A. Unwin, and S. Horn. Pattern recognition approach to identify natural clusters of acoustic emission signals. *Pattern Reco. Lett.*, 33:17–23, 2012.
- [11] JW Carmichael and RS Julius. Finding natural clusters. *Systematic Biology*, 17(2):144–150, 1968.
- [12] David L Davies and Donald W Bouldin. A cluster separation measure. *IEEE transactions on pattern analysis and machine intelligence*, (2):224–227, 1979.
- [13] Peter J Rousseeuw. Silhouettes: a graphical aid to the interpretation and validation of cluster analysis. *Journal of computational and applied mathematics*, 20:53–65, 1987.
- [14] Alexander Hohl, Adam D Griffith, Martha Cary Eppes, and Eric Delmelle. Computationally enabled 4d visualizations facilitate the detection of rock fracture patterns from acoustic emissions. *Rock Mechanics and Rock Engineering*, 51(9):2733–2746, 2018.
- [15] IA Rastegaev, DL Merson, AV Danyuk, MA Afanasyev, and A Vinogradov. Using acoustic emission signal categorization for reconstruction of wear development timeline in tribosystems: Case studies and application examples. *Wear*, 410:83–92, 2018.
- [16] I. Rastegaev, D. Merson, I. Rastegaeva, and A. Vinogradov. A time-frequency based approach for acoustic emission assessment of sliding wear. *Lubricants*, 52(7):1–24, 2020.
- [17] Shen-Bin Zhu, Zhen-Lin Li, Shi-Min Zhang, Le-Le Liang, and Hai-Feng Zhang. Natural gas pipeline valve leakage rate estimation via factor and cluster analysis of acoustic emissions. *Measurement*, 125:48–55, 2018.
- [18] MH Nagaraj, Johannes Reiner, R Vaziri, E Carrera, and M Petrolo. Progressive damage analysis of composite structures using higher-order layer-wise elements. *Composites Part B: Engineering*, 190:107921, 2020.
- [19] Ramesh Talreja and Chandra Veer Singh. *Damage and failure of composite materials*. Cambridge University Press, 2012.
- [20] Edward Kozłowski, Dariusz Mazurkiewicz, Tomasz Zabinski, Sławomir Prucnal, and Jarosław Sep. Machining sensor data management for operation-level predictive model. *Expert Systems with Applications*, 159:113600, 2020.
- [21] Stavros Ntalampiras. One-shot learning for acoustic diagnosis of industrial machines. *Expert Systems with Applications*, 178:114984, 2021.
- [22] Mohsen Motahari-Nezhad and Seyed Mohammad Jafari. Bearing remaining useful life prediction under starved lubricating condition using time domain acoustic emission signal processing. *Expert Systems with Applications*, 168:114391, 2021.
- [23] Edwin T Jaynes. Information theory and statistical mechanics. *Physical review*, 106(4):620, 1957.
- [24] Andrea De Martino and Daniele De Martino. An introduction to the maximum entropy approach and its application to inference problems in biology. *Heliyon*, 4(4):e00596, 2018.
- [25] L. Vendramin, R.J.C.B. Campello, and E.R Hruschka. Relative clustering validity criteria: A comparative overview. *Statistical Analysis and Data Mining*, 3(4):209–235, 2010.
- [26] Juhee Bae, Tove Helldin, Maria Riveiro, Sławomir Nowaczyk, Mohamed-Rafik Bouguelia, and Göran Falkman. Interactive clustering: a comprehensive review. *ACM Computing Surveys (CSUR)*, 53(1):1–39, 2020.

- [27] Emmanuel Ramasso, Benoit Verdin, and Gael Chevallier. Monitoring a bolted vibrating structure using multiple acoustic emission sensors: A benchmark. *MDPI DATA*, 7:31–45, 2022.
- [28] Physical Acoustics Corporation. Pic2 based AE system user’s manual, 2007.
- [29] William M Rand. Objective criteria for the evaluation of clustering methods. *Journal of the American Statistical association*, 66(336):846–850, 1971.
- [30] Quentin Lefebvre, Martial Personeni, Emmanuel Ramasso, and Sébastien Thibaud. Observation and detection of machining phases in edm microdrilling by acoustic emission. In *Structural Health Monitoring 2019: Enabling Intelligent Life-cycle Health Management for Industry Internet of Things (IIOT)*, pages 1–6, Stanford University, CA, USA, 2019.
- [31] Victor Giurgiutiu. *Structural health monitoring: with piezoelectric wafer active sensors*. Elsevier, 2007.
- [32] Donald E Gustafson and William C Kessel. Fuzzy clustering with a fuzzy covariance matrix. In *1978 IEEE conference on decision and control including the 17th symposium on adaptive processes*, pages 761–766. IEEE, 1979.
- [33] Neha Chandarana. *Combining passive and active methods for damage mode diagnosis in tubular composites*. PhD thesis, Manchester University, Faculty of Science and Engineering, Departement of Materials, 18th November 2019.

A Voting scheme algorithm

Algorithm 1 was proposed in [10].

```

1 Input: Matrix of features  $\mathbf{Y}$  with size  $N \times d$ ;
2 Input: The range of number of clusters  $[K_{\min}, K_{\max}]$ ;
3 Input: The subsets of features  $\mathcal{S}$ ;
4 Input: The set of weights for two voting schemes  $W_1, W_2$ ;
5 Output: Voted partition of the data  $P^*$ ;
6 Output: Clusters parameters  $\theta^*$ ;
7 for  $S \in \mathcal{S}$  do
8   for  $K \in [K_{\min}, K_{\max}]$  do
9     // Apply the clustering method and store the partition and parameters;
10     $[P(S, K), \theta(S, K)] \leftarrow \text{Clustering}(\mathbf{Y}(:, S), K)$ ;
11    // Quality can be evaluated with one or several indices;
12    // Indices used for AE are mostly internal and focus on clusters shape;
13     $Q_{\text{literature}}^{\text{SHAPE}}(S, K) \leftarrow \text{Internal\_Shape\_Indices\_Quality}(P, Y(:, S), \theta)$ ;
14  end
15 end
16 // For each subset, firstly find the clusters using a voting scheme;
17 // The vote uses weights set a priori by the end-user;
18 for  $S \in \mathcal{S}$  do
19    $\text{nb\_clusters}(S) \leftarrow \arg \max_k \text{Vote}(Q(S, k), W_1)$ ;
20 end
21 // Then find the subset and the final number of clusters using a second voting scheme;
22  $S^* \leftarrow \arg \max_S \text{Vote}(Q(S, \text{nb\_clusters}(S)), W_2)$ ;
23  $K^* \leftarrow \text{nb\_clusters}(S^*)$ ;
24 // Return results;
25  $P^* \leftarrow P(S^*, K^*)$ ;
26  $\theta^* \leftarrow \theta(S^*, K^*)$ ;

```

Algorithm 1: Evaluation of clustering methods: Shape-based *internal* indices with voting scheme used in the literature [10]. The output partition is on selected by a vote from the subset of partitions generated by clustering.

B Onset-based algorithm

```

1 Input:      Matrix of features  $\mathbf{Y}$  with size  $N \times d$ ;
2 Input:      The range of number of clusters  $[K_{\min}, K_{\max}]$ ;
3 Input:      The subsets of features  $\mathcal{S}$ ;
4 Output:     Histogram of onsets;
5 for  $K \in [K_{\min}, K_{\max}]$  do
6   for  $S \in \mathcal{S}$  do
7     // Apply the clustering method and store the partition and parameters;
8      $[P(S, K), \theta(S, K)] \leftarrow \text{Clustering}(\mathbf{Y}(:, S), K)$ ;
9     // Compute quality according to how onsets are distributed;
10     $Q_{\text{proposed}}^{\text{ONSETS}}(S, K) \leftarrow \text{Onsets\_Clusters\_Quality}(P)$ ;
11  end
12  // Sort and select a few subsets of subsets of features for each  $K$  using Eq. 9. The threshold can be adapted
    according to the number of subsets considered;
13   $q_{0.99} = \text{quantile with probability } 0.99 \text{ of } Q_{\text{proposed}}^{\text{ONSETS}}(S, K)$ ;
14   $S_{\text{sub}}(K) = \{S : Q_{\text{proposed}}^{\text{ONSETS}}(S, K) \geq q_{0.99}\}$ ;
15  // Find onsets of the selected partitions;
16   $\text{Onsets}(K) = \text{Find\_onsets}(F(K))$ ;
17 end
18 // Accumulate evidence from various numbers of clusters using histogram;
19 // The number of intervals in the histogram depends on the application;
20  $\text{Acc} = \text{Histogram}(\text{Onsets}(\forall K))$ ;
21 // Present the histogram to the end-user who can then either reject, accept, or be ignorant of the result, triggering a
    re-clustering of the data [26].;
```

Algorithm 2: Onsets-based algorithm using Eq. 9 by evidence accumulation.